

A TRAPPED MERCURY 199 ION FREQUENCY STANDARD

Leonard S. Cutler, Robin P. Giffard, and Michael D. McGuire
Hewlett-Packard Laboratories, Palo Alto, California

ABSTRACT

Mercury 199 ions confined in an RF quadrupole trap and optically pumped by mercury 202 ion resonance light form the basis for a high performance frequency standard with commercial possibilities. This report describes some results achieved to date and gives estimates of the potential performance of such a standard.

DESCRIPTION OF STANDARD

The mercury 199 ion has a number of desirable properties for a hyperfine frequency standard (1-3). It is massive and thus has relatively small, second order doppler shift. The hyperfine frequency is 40.5 GHz, high enough to give good line Q but not so high as to be very difficult to generate. The nuclear spin is 1/2 so the hyperfine levels, F=0 and F=1, have only one and three states respectively, and the transition between the m=0 levels has no first order magnetic field dependence. Since the hyperfine frequency is high, the second order magnetic field dependence is small, allowing good performance with relatively simple shielding. A simple optical pumping and detection scheme exists.

The energy levels of the mercury 199 and 202 ions are shown in Fig. 1 (2). Mercury 202 has no nuclear spin and consequently no hyperfine structure. The transition between its ionic ground state and the first excited state matches fairly well the transition between the F=1 level in the mercury 199 ion and its first excited states at a wavelength of 194.2 nm. Consequently 199 ions will be pumped from the F=1 level to the excited states from which they will decay back to both ground state levels. In the absence of relaxation they would all end up in the F=0 level. A sample of ions so pumped would become transparent to the pumping radiation and the fluorescence would vanish. Microwave radiation at the resonance frequency between the F=0 and F=1 levels would repopulate the F=1 level, making ions available for pumping and producing fluorescence. Observation of this fluorescence can thus be used to detect the hyperfine resonance.

The ions must have a long lifetime if they are to have a narrow linewidth. This is accomplished by using an RF quadrupole trap. Neutral mercury 199 inside the trap is bombarded with an electron beam to form ions which will stay in the trap if the potentials and drive frequency are suitable. Lifetimes of many seconds in the trap are easy to achieve. It is possible to store of the order of $1E6$ ions. First order doppler shift in the trap averages to zero and the broadening can be kept under control.

With this number of ions and typical pumping intensities, the fluorescence and stray background levels are low enough for photon counting to be used. This simplifies the electronics since mostly digital circuitry can be used.

Fig. 2 is a schematic diagram of a standard on which we have been working. The trap is shown being illuminated with a focused and filtered light beam from the mercury 202 lamp. The fluorescence from the mercury 199 ions in the trap is collected by the optics at right angles to the input beam and focused into the photomultiplier tube. Since the incident and fluorescent light have the same wavelength, great care must be exercised to keep the stray, scattered light to a minimum. The output pulses from the photomultiplier are fed to a counter whose gate is controlled by the sequencer.

The operations the sequencer performs are shown in Fig. 3. After an interval of optical pumping the light is turned off and the ions are irradiated with the microwave frequency tuned to one side of the line. The microwaves are then turned off, the pumping light applied again, and the counter gate is opened for a time. After the gate is closed the electron beam is turned on for a short time to refresh the ion population. The whole process is then repeated with the microwave frequency tuned to the other side of the line. If the mean frequency of the microwave source, as it is switched between the two sides of the line, is not at the line center, there will be a difference in the counter readings which is used as the error signal for the mean frequency. The counter readings are differenced and digitally integrated by the computer and then converted to an analog signal. A second integration is performed and the control signal is fed to the VCXO and synthesizer. The double integration eliminates the effects of linear frequency drift in the flywheel oscillator. It also removes the effect of frequency jumps in the flywheel oscillator on time kept by the standard when it is used as a clock.

The light is switched off during the time the RF is applied to avoid light induced frequency shift and line broadening. The electron beam is also switched off to avoid its line broadening effect and to remove the electron induced fluorescence.

Rather than using first differences as the error signal, second differences are used. This removes any error due to linear drifts in system parameters such as light intensity, ion number, etc. The second differences are formed by the computer as follows. Consider a sequence of counts from the system

$$C_1, C_2, C_3, C_4, \dots$$

The computer forms the sequence

$$+(C_1 - 2C_2 + C_3), -(C_2 - 2C_3 + C_4), +(C_3 - 2C_4 + C_5), \dots$$

It is easy to show that each member of this sequence contains the error information and removes linear parameter drifts. This is similar to the scheme used by Jardino et al (3) and gives, in addition, new error information for each count, thus allowing faster loop response.

Some other aspect of the system should be mentioned. The mercury 202 lamp is excited by RF at a level of about 20 watts. Its intensity is controlled by a photodiode monitor feedback loop. The present microwave source is a phase-locked Gunn diode. For making measurements the system is operated open-loop with the VCXO phase-locked to a cesium standard. Most of the measurements reported here were done in this mode. Optical design is critical to achieving good signal to noise ratio. The design of the input and output light paths strives to maximize the ion fluorescence signal while minimizing stray light, which at present is the largest photon flux at the photomultiplier. The present experimental arrangement has no magnetic shields. The ambient field is partially cancelled with sets of Helmholtz coils and gradient coils. Fields as low as 10 mG have been achieved but with questionable homogeneity.

The most important source of frequency shift is the second order doppler effect. This is given approximately by the ratio of the average kinetic energy of the ions in the trap to their rest energy. For mercury 199 the shift amounts to $-5.4 \text{ E-}12$ per eV of kinetic energy. The energy of uncooled ions in a trap (4) is typically about one tenth the well depth or about 2.0 eV. Since the effect is second order in velocity it can also induce line asymmetry if there is a distribution of velocities. Another effect of the velocity distribution is line broadening. Consequently it is almost essential to cool the ions.

Laser cooling is very effective (5) but not attractive from a commercial standpoint. The approach under investigation here uses viscous drag cooling (6) in which the hot ions are cooled by making collisions with a cool, light, inert gas such as helium. Calculations show that effective cooling should take place at gas pressures as low as about 1 E-6 torr. There is also a frequency shift due to the collisions with the cooling gas, but this should be small at the low pressures involved. More will be said about this later.

MEASUREMENTS

A large number of measurements have been made during the course of the work. The experimental setup includes a small computer that can control many of the operating parameters and also collect and store data. Many of the experiments involve data gathering overnight or over a week-end.

Fig. 4 shows a line recorded overnight. In this case the sequence was one which allowed the RF irradiation and optical pumping to come into equilibrium before the fluorescence count rate was measured, resulting in a conventional CW lineshape. The FWHM is 1.55 Hz. The ambient field was 0.52 gauss. There was helium present at about 2E-6 torr. The line was swept 32 times at 16 seconds per point, and the resulting set of points is the average of all the 32 sets. The fitted curve is a Lorentzian line with free parameters height, width, and center frequency. The background was subtracted out by taking alternate measurements with the frequency far removed from the resonance.

Fig. 5 shows a pulsed line recorded overnight. The ambient field was 0.46 gauss and helium was present. The line was swept 60 times at 8 seconds per point and the resulting data is the average of the 60 sets of points. The valleys are due to the pulsed operation. The length of the RF pulse was 0.24 seconds. Again, the background has been subtracted out. The effective linewidth is about 3.5 Hz.

Fig. 6 shows a pseudo-derivative of the pulsed line. Conditions were approximately the same as those for Fig. 5. It was obtained by sweeping slowly through the resonance while the frequency was being switched back and forth 3.5 Hz. The difference in counts for the two conditions is plotted as a function of the average frequency and, of course, goes through zero at line center. This is very close to the actual discriminator action to be used in the operating standard. This plot also is the result of averaging over a long run.

Fig. 7 shows the effect of trap well depth variation on zero magnetic field ion resonance frequency. As mentioned earlier the mean kinetic energy of the ions in the trap has been reported to be about one tenth the well depth. This should lead to a second order doppler shift of -0.022 Hz per eV of well depth. The depth was varied by changing the trap drive voltage and was calculated from the harmonic oscillator model using measured motional resonance frequencies for the ions. The hyper-fine resonance frequency data shown in Fig. 7 were taken with the best vacuum attainable in the system at that time. This was about $1 \text{ E-}7$ torr indicated and the system probably contained some residual helium. The straight line with slope -0.022 Hz per eV that is the best fit to the data points is shown. Each data point is the mean of five measurements and the standard deviation of that mean is about 0.01 Hz. This is about half the height of the crosses. The departures from the straight line are much larger than the standard deviation and must represent real variations from the simple straight line model. This behavior is not understood and more work is needed.

Some measurements were made of the dependence of frequency on helium pressure. Only a few results have been obtained thus far. One experiment was to measure the frequency as the helium pressure was slowly increased from the best vacuum attainable to about $5 \text{ E-}6$ torr. The frequency changed less than $2 \text{ E-}12$. This is a surprising result that could possibly be explained by a fortuitous cancellation of two effects: the second order doppler shift reduction induced by the helium cooling and the shift due to the helium. Another experiment involved varying the trap well depth as described earlier but with helium present at a pressure of $5 \text{ E-}6$ torr. The change in frequency was plus or minus $3 \text{ E-}13$ for a well depth change from 17.5 to 23.2 eV. This change is much smaller than the vacuum results and indicates that the helium cooling is effective. Other effects of the helium include narrower lines and a larger signal indicating cooling and perhaps storage of more ions. The gas technique for cooling is promising but needs more work.

The resonance line was studied as a function of the static magnetic field. As mentioned earlier, the apparatus is unshielded and the homogeneity of the field is questionable. At fields lower than about 70 mG the line became broadened, distinctly non-Lorentz shaped, and quite sensitive to externally applied gradients. Zeeman transitions were also observed. They were fairly broad and also indicated the presence of small amounts of low frequency AC magnetic field, most probably from the 60 Hz power lines and rotating machinery.

Measurements were also made of the effective signal to noise ratio for the pulsed mode of operation. The results would give a square root of the Allan variance of

$$\sigma_y(2, \tau) = 1.2 \text{ E-}12 (\tau)^{-1/2}$$

for times longer than the servo time constant. Due to the narrow line and the consequent slow data gathering rate, this time constant is presently about 20 seconds.

Measurements were made of relaxation and pumping rates. In the notation of Jardino and Desaintfusien (2) a set of measurements was:

$$\begin{aligned} \gamma_p &= 1.8 \text{ sec}^{-1} \\ \gamma_1 + \gamma_s &= .43 \text{ sec}^{-1} \\ \Gamma_2 &= 4.9 \text{ sec}^{-1} \end{aligned}$$

γ_p = pumping rate

γ_s = (storage time)⁻¹

γ_1 = longitudinal relaxation rate

Γ_2 = total transverse relaxation rate

These do not necessarily represent the best conditions for frequency standard operation.

The background photon count rate depends strongly on a number of factors. The contributions to background are stray light scattered from the incident beam, atomic fluorescence from the background gas, residual fluorescence from the ions due to relaxation, and light from the heated electron gun. The electron beam is switched off during counting so there is no electron induced fluorescence. The background count rate also, of course, depends on the available light. For the line shown in Fig. 4 the background count rate was 11,500 per second while the signal count rate was 3,250 per second at a saturation factor of 3.2. Background rates of 1.5 E5 with signal rates of about 1.7 E4 have also been observed.

An estimate of the absolute hyperfine frequency in zero magnetic field and with zero second order doppler shift based on the results of Fig. 7 is

$$= 40,507,347,996.9 \pm 0.3 \text{ Hz}$$

The uncertainty is mainly due to the extrapolation to zero second order doppler shift. The uncertainty due to the cesium standards used as reference is no larger than 0.1 Hz referred to NBS. Measurements made with 4E-6 torr of helium are slightly lower in frequency but still fall within the quoted uncertainty range.

REFERENCES

1. F. G. Major and G. Werth; *Appl. Phys.* 15, 201 (1978).
M. D. McGuire, *Proceedings of the Frequency Control Symposium 1977*, p 612.
2. M. Jardino and M. Desaintfusicien; *IEEE Trans. Inst. Meas.* IM29, 163 (1980).
3. M. Jardino, M. Desaintfusicien, R. Barillet, J. Viennet, P. Petit, and C. Audoin, *Appl. Phys.* 24, 107 (1981).
4. R. Ifflaender and G. Werth; *Metrologia* 13, 167 (1977).
5. W. Neuhauser, M. Hohenstatt, P. E. Toschek, H. G. Dehmelt; *Appl. Phys.* 17, 123 (1978).
D. J. Wineland, R. E. Drullinger, and F. L. Walls; *Phys. Rev. Lett.* 40, 1639 (1978).
6. F. G. Major and H. G. Dehmelt, *Phys. Rev.* 170, 91 (1968).
H. Schaaf, U. Schmeling, and G. Werth; *Appl. Phys.* 25, 249 (1981).

Measurements of stability of the mercury standard against a high performance cesium standard were made with averaging times of 100 sec. The measured fluctuations were essentially those of the cesium, at a level of 5 E-13 . The mercury standard fluctuations were not detectable.

CONCLUSIONS

The optically pumped trapped mercury ion frequency standard looks promising. A number of measurements have been made to ascertain its potential. While a great deal of work remains to be done, it appears that the following performance characteristics could be met in a commercial standard:

absolute accuracy	1 E-12
Reproducibility	2 E-13
$\sigma_y(2,\tau)$	$1 \text{ E-12 } (\tau)^{-1/2}$

ACKNOWLEDGMENTS

The authors are grateful for useful discussions with Dr. C. Audoin and Dr. M. Desaintfuscien and for preprints they and Dr. M. Jardino have sent. Construction of much of the electronics was carried out by D. Weigel.

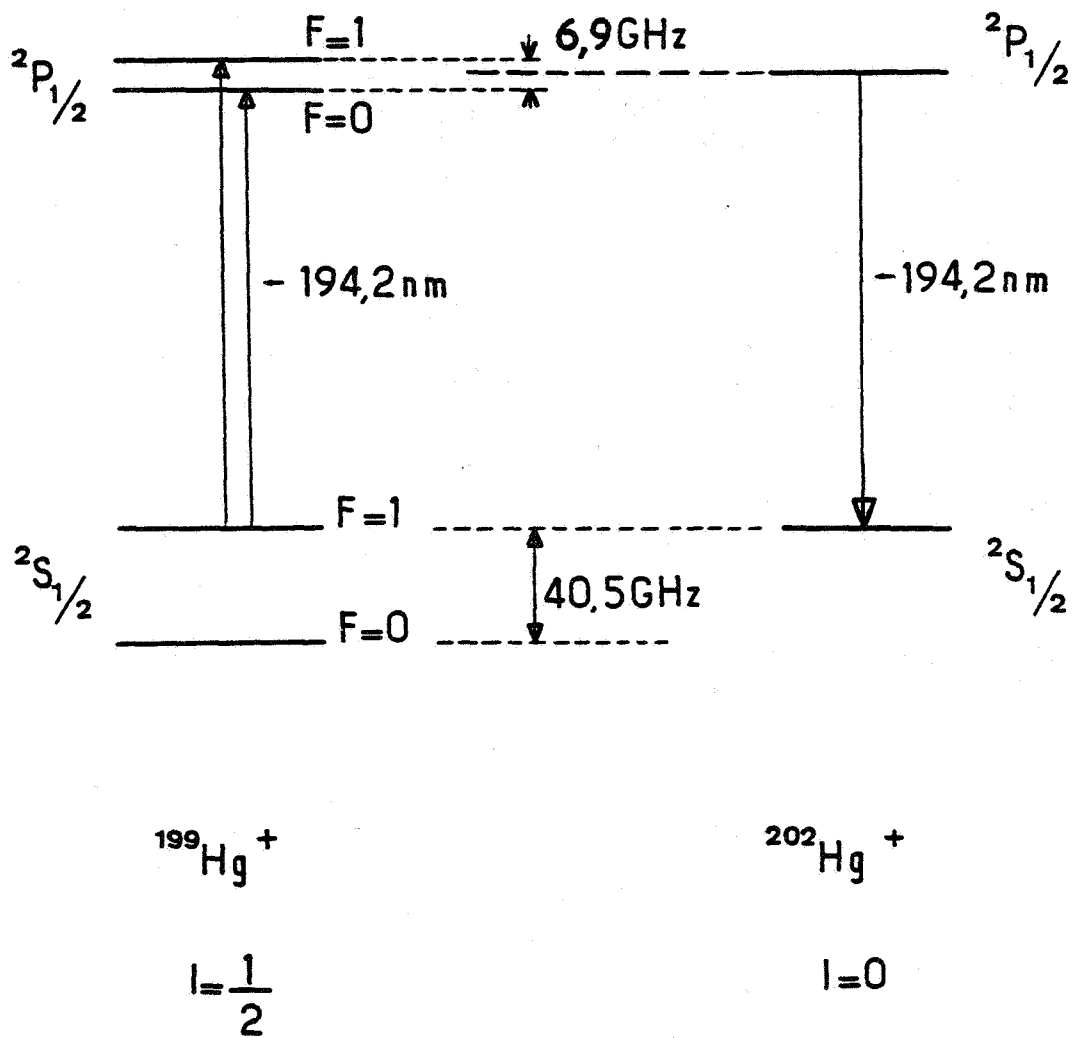


Fig. 1 - Energy levels of mercury 199 and 202 ions.

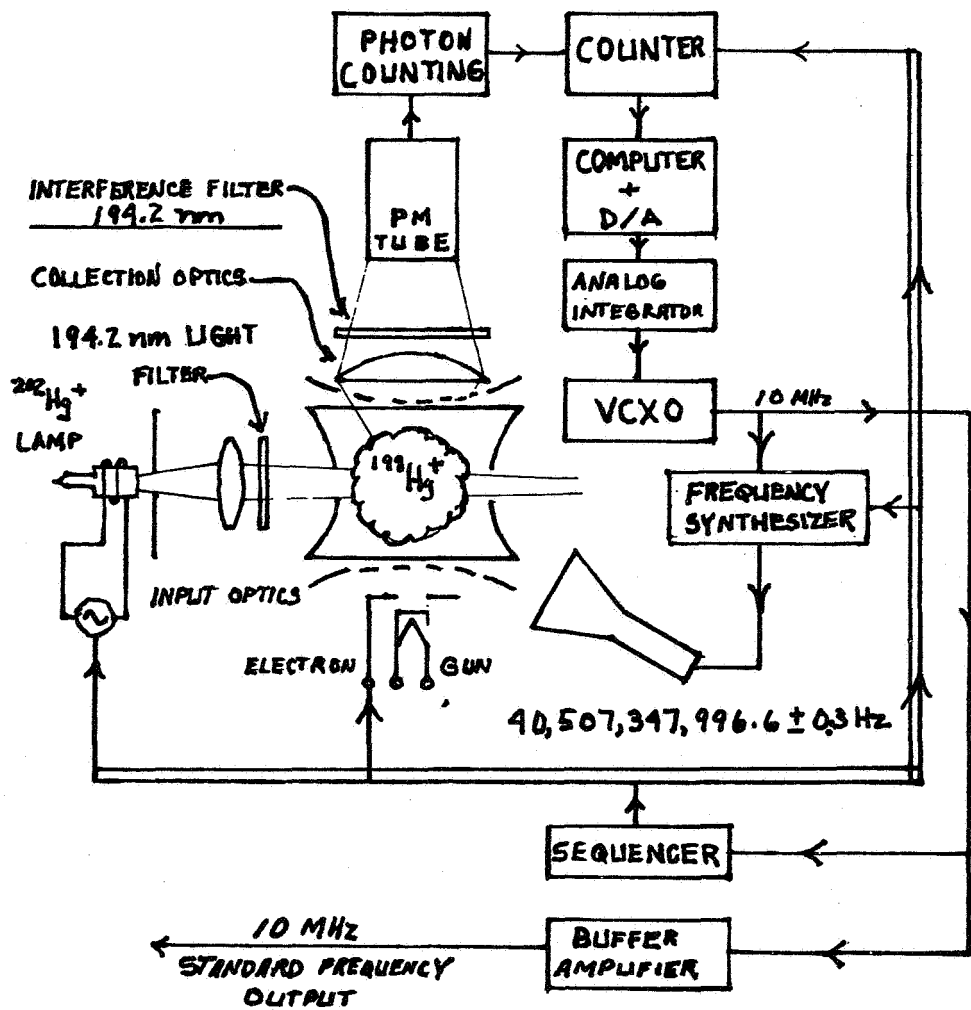


Fig. 2 - Schematic diagram of trapped mercury ion standard.

MEASUREMENT SEQUENCE

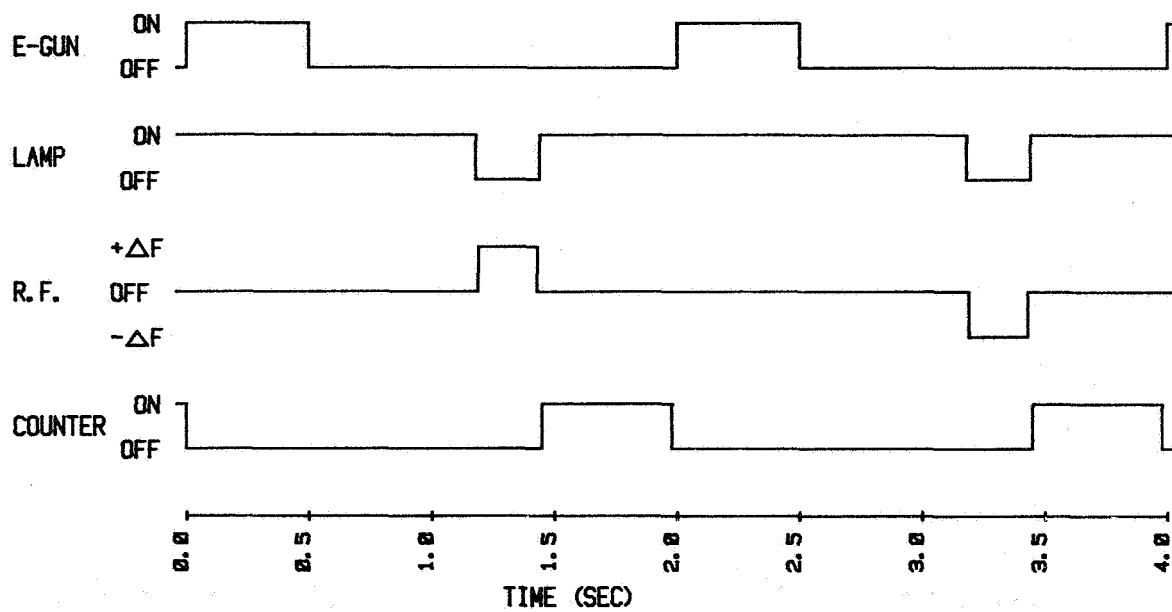


Fig. 3 - Sequencer Operation

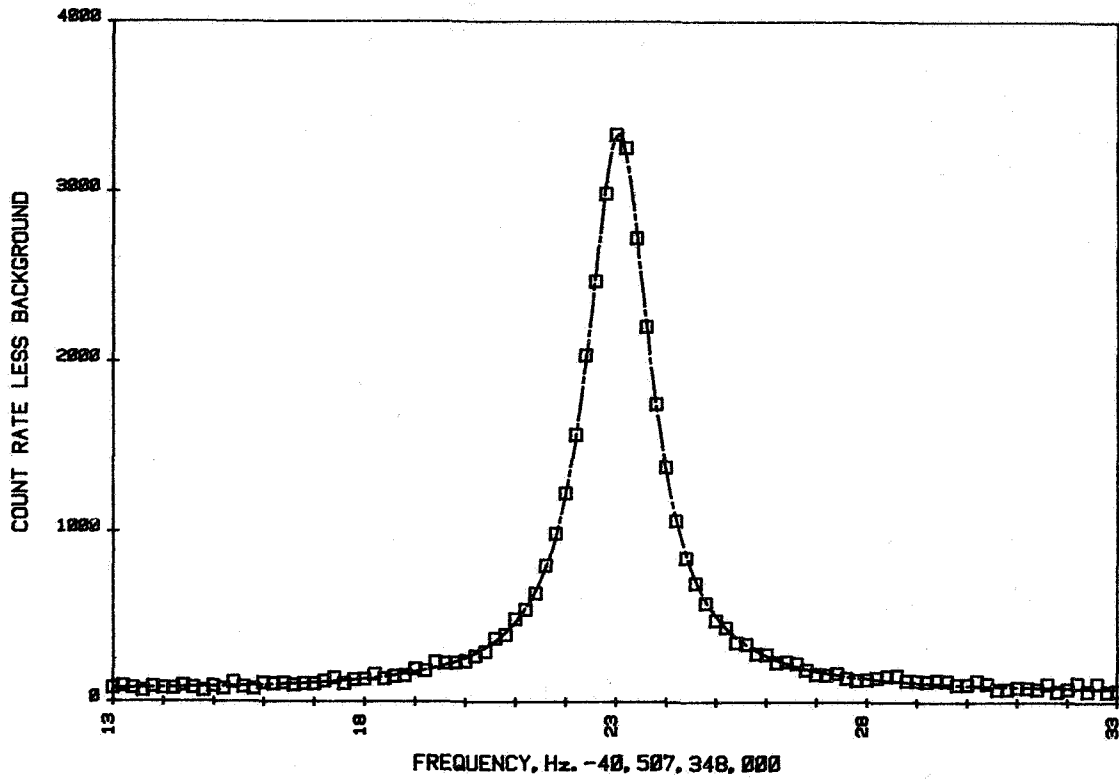


Fig. 4 - CW line with helium. FWHM is 1.55 Hz. The fitted curve is a Lorentz line.

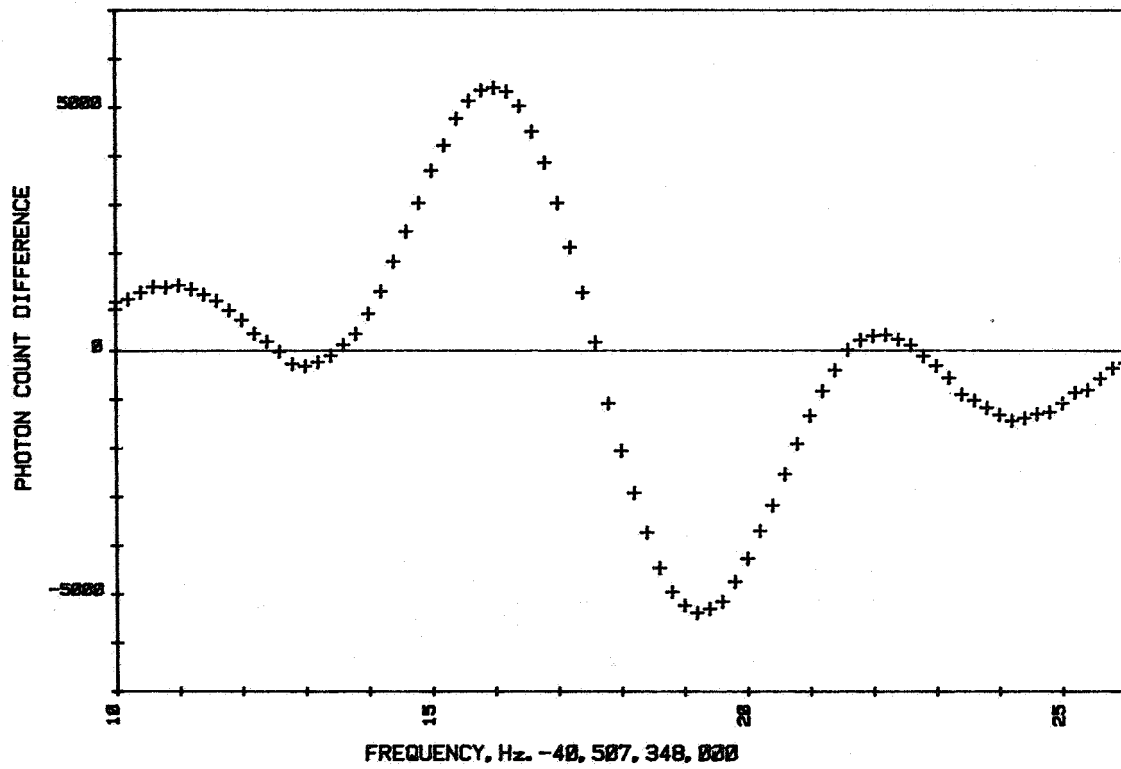


Fig. 6 - Pulsed line pseudo-derivative. This is a first difference error signal.

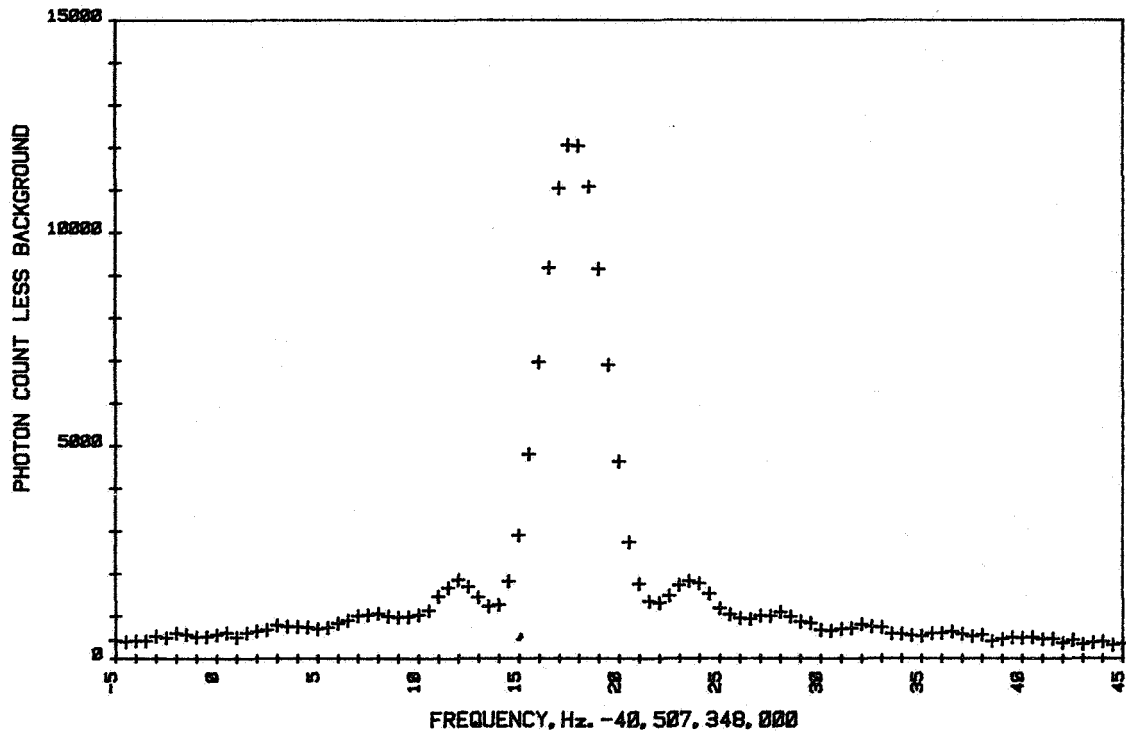


Fig. 5 - Pulsed line. The RF pulse width is 240 ms.
FWHM is about 3.5 Hz.

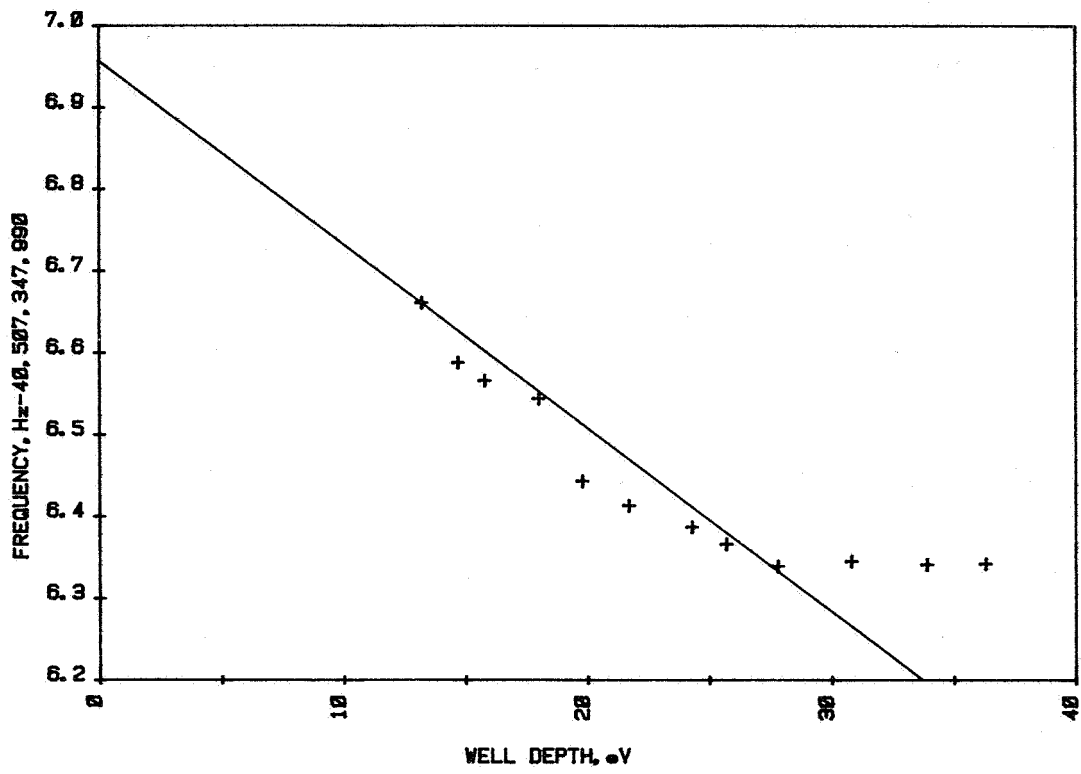


Fig. 7 - Hyperfine resonance frequency versus trap well depth. Standard deviation of each data point is less than 0.01 Hz. The straight line slope corresponds to second order doppler shift for ion energy equal to 0.1 well depth. Data points are corrected to zero magnetic field.